Original Article

Quantitative measurement of cutaneous neurofibromas in neurofibromatosis type 1 using a structured-light scanner

Tabea Isabelle Hartung[1]^, Güren Tan Dinga[1,2], Jonas Butschan[1], Lan Kluwe[1]^, Said Chosro Farschtschi[1]^

[1]Department of Neurology, University Medical Center Hamburg-Eppendorf, Hamburg, Germany; [2]Lab for Geoinformatics and Geovisualization, HafenCity University Hamburg, Hamburg, Germany

Contributions: (I) Conception and design: All authors; (II) Administrative support: TI Hartung, SC Farschtschi; (III) Provision of study materials or patients: SC Farschtschi; (IV) Collection and assembly of data: TI Hartung, GT Dinga, J Butschan, L Kluwe; (V) Data analysis and interpretation: TI Hartung, J Butschan, L Kluwe; (VI) Manuscript writing: All authors; (VII) Final approval of manuscript: All authors.

Correspondence to: Dr. Tabea Isabelle Hartung, MD. Department of Neurology, University Medical Center Hamburg-Eppendorf, Martinistr. 52, 20246 Hamburg, Germany. Email: t.hartung@uke.de.

Background: Cutaneous neurofibromas (cNF) are found in >99% of adults with neurofibromatosis type 1 (NF1) and are a hallmark feature of the disorder. Due to the large number, varying sizes, and irregular distribution of the tumors, quantification is hardly possible for most cases. We introduce a novel structured-light scanner to address this issue.

Methods: This NF-scanner captures the three-dimensional (3D) geometry of neurofibromas in patients and calculates the number, area, and volume of the tumors over the whole body. The measuring time is about 7 minutes for most cases. Validation was performed on 100 model neurofibromas (hemispheres, diameters 6–20 mm) affixed to a standardized torso model in two spatial distributions (evenly distributed and clustered), with five repeated measurements per configuration. Subsequently, the scanner was applied to 16 patients with NF1 (eight male and eight female; age range, 19–69 years), each undergoing three to six repeated whole-body scans. Intra-individual measurement variability was quantified using coefficients of variation, and the correlation of tumor burden parameters with age was assessed using Spearman's rank correlation.

Results: Testing on modelled neurofibromas demonstrated reproducibility for number and area measurements. For evenly distributed model neurofibromas, the scanner detected a mean count of 131 (true value: 100; overestimation approximately 31%), with measured total area and volume corresponding to 96% and 65% of the true values, respectively. For clustered model neurofibromas, mean detection yielded 83.8 lesions (approximately 16% underestimation), with total area and volume at approximately 80% and 53% of ground truth. Clinical application in 16 patients confirmed the expected correlations of age with number, total area, and total volume of the tumors. Neurofibroma counts ranged from 500 to more than 2,700 per individual. Tumor number, total area, and total volume all showed significant positive correlations with patient age. Intra-individual coefficients of variation were lowest for tumor count and highest for total volume, indicating that surface-based parameters are more robustly reproducible than volumetric estimates with the current analysis pipeline.

Conclusions: The NF-scanner enables quantification of neurofibromas in a large number of patients, and therefore contributes to improving clinical documentation and clinical research. Tumor count and total area measurements demonstrated acceptable reproducibility, whereas volumetric assessments showed greater variability, consistent with findings from comparative studies of other 3D imaging systems. With further refinement of the analysis software, the structured-light NF-scanner offers a scalable, contact-free

^ ORCID: Tabea Isabelle Hartung, 0009-0007-5463-0971; Lan Kluwe, 0000-0001-9919-4551; Said Chosro Farschtschi, 0000-0002-3596-5932.

approach for objective whole-body quantification of cNF burden, suitable for both clinical documentation and interventional research.

Keywords: Neurofibromatosis type 1 (NF1); structured-light three-dimensional scanner (structured-light 3D scanner); cutaneous neurofibromas (cNF); quantitative measurement

Submitted Jan 08, 2026. Accepted for publication Apr 09, 2026. Published online Apr 30, 2026.
doi: 10.21037/qims-2026-1-0053
View this article at: https://dx.doi.org/10.21037/qims-2026-1-0053

Introduction

Neurofibromatosis type 1 (NF1) is an autosomal dominantly inherited disorder with an incidence of approximately 1 in 3,000 newborns (1) and is characterized by a broad spectrum of clinical manifestations, including café-au-lait macules, bilateral freckling, and neurofibromas (2). Cutaneous neurofibromas (cNF) are benign tumors, originating from Schwann cells and manifesting primarily as skin nodules, which can significantly impact patients' quality of life (3-6). These tumors are found in >99% of adults with NF1 (7), usually appear in adolescence, increase in age, and often show rapid growth in puberty and during pregnancy (7-9).

Magnetic resonance imaging (MRI) and MRI-based volumetric assessment of tumors have been employed to evaluate growth patterns of internal plexiform neurofibromas and other NF1-related tumors (10-12). However, these techniques are less practical for routine and repeated assessment of cutaneous lesions. In addition, MRI does not accurately measure very small surface tumors and is severely influenced by artifacts depending on body position and skin compression. To date, photographs and manually counting are the most applied approaches in clinical documentation (13,14). However, these methods are inaccurate, show a significant interrater variation, and are extremely labor-intensive (15,16). Several imaging-based approaches have been explored for the objective assessment of cNF in patients with NF1. Recently, imaging techniques including high-frequency ultrasound and three-dimensional (3D) imaging have been evaluated and shown improved reliability for the documentation and monitoring of cNF lesions (16,17). Comparative studies of different 3D imaging systems further demonstrate high reproducibility for surface-based measurements such as lesion area, although volumetric assessments may show greater variability between devices (18). These developments highlight the growing need for standardized and efficient imaging approaches that allow objective and large-scale quantification of cNF burden in clinical research (19).

Despite these advances, many currently available techniques remain limited to the assessment of selected lesions or restricted body areas and are often time-consuming when large numbers of tumors are present. Considering that patients with NF1 may develop hundreds to thousands of cNF, efficient methods enabling rapid and objective whole-body quantification remain an unmet need in both clinical practice and research (19). To address this challenge, we evaluated a structured-light 3D scanning system designed to capture the entire body surface and automatically quantify the number, area, and volume of cNF.

Structured light scanning is based on 3D scanning technology that can capture shapes and dimensions of objects by projecting a series of light patterns, such as fringes, grids, or stripes, onto the object's surface (20). The deformation of the projected patterns is captured by one or multiple cameras, which allows the scanner to reconstruct the geometry in 3D (21,22). 3D scanners can measure surfaces and objects with sub-millimeter precision to transfer them into digital 3D models in real time. Mainly used in industrial inspection for the accuracy of manufactured parts as well as reverse engineering of existing objects for redesign, optical 3D scanners are also used in healthcare, e.g., for prosthesis fitting and plastic surgery (23-25). Due to the high accuracy and the almost instantaneous recording of objects, 3D scanners are very well suited for *in vivo* measurements on patients (AICON 3D Systems, 2015).

We studied the feasibility of this 3D scanner for measuring cNF in NF1 patients. The AEVA-HE (EOTECH SAS, Marcoussis, France) neurofibroma scanner was specifically designed for our aim. After an initial validation on model neurofibromas, we carried out real measurements on 16 patients with NF1. We present this article in accordance with the STARD reporting

checklist (available at https://qims.amegroups.com/article/view/10.21037/qims-2026-1-0053/rc).

Methods

The study was conducted in accordance with the Declaration of Helsinki and its subsequent amendments. The study was approved by the ethics committee of Ärztekammer Hamburg, Germany (Nos. 2022-300264-WF and 2022-100983-BO-ff), and informed consent was taken from all individual participants.

Structured-light 3D scanner

The vertically mounted AICON smartSCAN-HE scanner projector uses a 50-W LED lamp to project series of light-patterns onto the object. These patterns consist primarily of alternating dark and light vertical stripes. Two AVT Pike F-505B cameras measure the change of light-patterns and calculate 3D coordinates for each captured pixel captured. Three additional LED lamps flooding the scene to take a color image with a Canon 1200D DSLR to create textures for the 3D model if needed. The patient stands on a turning table which rotates 45° for eight times to enable eight measurements from different directions. The overlapping measuring data is then merged into a single 3D body model. Upon completion of the eight measurements, the scanner moves down automatically by 50 cm and repeats the above procedure. With three vertical movements, each with eight rotations, the entire body of a patient is captured in close to 7 minutes. Custom-engineered software on the AICON-Platform was used to enable direct processing of 3D models for analysis, resulting in a 3D model highlighting detected cNF. Output data included count, area, and volume. For each patient, five consecutive measurements were performed.

Model neurofibromas

A total of 100 hemispheres with diameters ranging from 6 to 20 mm made of wood (*Figure 1A*) were attached to a torso covered in material which diffusely reflects light and therefore mimics skin (*Figure 1*). The model neurofibromas are either evenly *(Figure 1B*) or clustered (*Figure 1C*) distributed. For each torso, the measurement was repeated five times, and the results were compared with the real data.

Patients

A total of 16 (eight male and eight female) patients aging from 19 to 69 years were recruited from our Neurofibromatosis Outpatient Clinic at the University Medical Center Hamburg-Eppendorf, Hamburg, Germany between February and May 2023. All participants provided informed consent for study participation, and data processing was performed in a fully anonymized manner. The diagnosis of NF1 was according to the established criteria (2). The patient characteristics and measurement data are summarized in *Table 1*. For the measurement, clothes were taken off except the underpants. Due to the formation of wrinkles in underpants, which can lead to misinterpretation by the analysis software as fibromas, this region was not considered for analysis. The same applies to the area above the neck. In total, approximately 75% of the total surface area could be analysed. The area of cNF was normalized by dividing with the total body surface area. Each patient underwent three scans in succession. Four participants were rescanned after 2 to 3 months.

Results

Measurement on model neurofibromas

For the 100 evenly distributed model neurofibromas (*Figure 1A*,*1B*,*1D*,*1E*), the averaged count from the five measurements was 131. The averaged area and volume of the model neurofibromas were 96% and 65% of the real ones, respectively (*Figure 2A*, *Table 2*).

For the 100 clustered model neurofibromas (*Figure 1C*), the scanner identified 83.8 at average from the five measurements. The averaged total area and volume were approximately 80% and 53% of the real values, respectively (*Figure 2B*, *Table 3*).

Measurement on 16 patients

Each patient was measured three or six times at 1 or 2 measurement days in an interval of 2 to 3 months. At each appointment, the measurement was repeated five times. Detected neurofibromas by the scanner are demonstrated in three cases (*Figure 3*). From the total of 15 or 30 measurements for each patient, the averaged number, density, total area, area/tumor, total volume, and volume/tumor of the neurofibromas were calculated. Number of neurofibromas per patient varied from 500 to more than

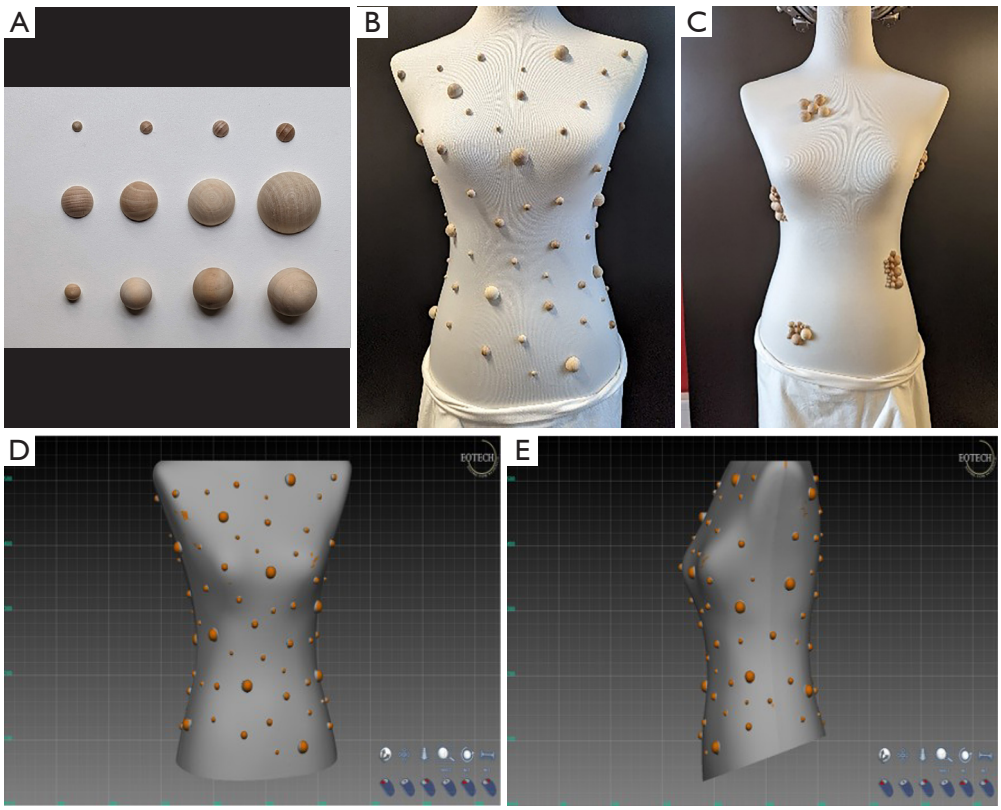

Figure 1 Model neurofibromas on torsos. (A) Hemispheres made of wood with diameters from 6 to 20 mm, mimicking neurofibromas; (B) evenly distributed hemispheres; (C) clustered hemispheres; (D,E) detected and marked hemispheres by the scanner. The torsos were covered with material which diffusely reflects light.

2,700. The results are summarized in *Figure 4*.

Tumor number, total area, and total volume were all correlated with age (*Figure 5*). No significant difference was found between male and female patients.

Variation coefficients of these parameters among the 3 to 6 measurements were calculated for each patient (*Figure 6*). Total volume had the highest variability, followed by total area, density, and number. The relatively low variation coefficients for tumor number and total area indicate good repeatability of the scanning method across repeated measurements, whereas total tumor volume showed higher variability. These findings suggest that surface-based parameters such as tumor count and area can be measured more robustly than volumetric estimates with the current analysis pipeline.

Discussion

Our study introduces a novel measurement tool for quantifying neurofibromas using a 3D scanner. After validating on model neurofibromas, the measurement was carried out on 16 patients.

Measuring evenly distributed model neurofibromas resulted in an approximately 30% overestimation, which is within the range we expect to be clinically significant in MRI (26). One cause is that some structures on the torso other than the hemispheres are misinterpreted by the software as such (*Figure 7A*). This problem is more pronounced in real patients, since movement during the measurement also causes artifacts. Another cause for the overestimation is the "double counting", where a hemisphere is captured in full and as a smaller fragment (*Figure 7B*). In contrast to the overestimations in number, the total area and volume is generally less than the real one. The major reason is the incomplete capture of the hemisphere, which does not go down to the surface (*Figure 7C*). In the clustered case, the hemispheres with contact with each other are counted as a single one

Table 1 Patient: demographic information, number of scans, body metrics (weight and height), and key cNF characteristics (average number, density, area, and volume)

Patient	Age (years)	Gender	Number of scans	Weight (kg)	Body height (cm)	Average number of cNF	cNF density (%)	Average area (mm^2)	Area (mm^2)/cNF	Average volume (mm^3)	Volume (mm^3)/cNF
5311	19	M	3	81	172	738	2.3	20,102	27.2	2,079	2.8
1500	24	F	3	58.2	164	500	2.04	15,192	30.32	1,712	3.39
1410	25	M	6	61.9	167.5	985	3.65	28,531	28.86	2,460	2.49
3174	26	M	3	68.1	168	765	2.5	23,467	30.7	2,592	3.4
5609	28	M	6	63.5	182	1,053	4.6	33,497	31.8	3,963	3.8
1476	33	M	3	82	173	840	2.67	25,179	30.05	2,716	3.27
3680	34	F	3	45.5	152.8	870	4	27,879	32.1	4,488	5.2
5369	36	M	3	80.5	168	645	2	17,054	26.4	1,302	2
5186	40	F	3	61.5	163	616	2.2	19,285	31.3	3,283	5.3
5936	40	F	6	58.8	170	1,263	4.7	38,673	30.6	5,874	4.6
3877	46	M	3	109.2	178	2,029	8.5	65,711	32.4	9,952	4.9
7287	47	F	6	88.5	172	2,787	7.7	91,603	32.9	17,144	6.1
7653	52	F	3	62.1	159	1,310	5.4	44,195	33.7	9,948	7.6
1136	55	M	3	73	170	862	2.83	27,280	31.7	3,442	3.99
6765	56	F	6	64.1	153	1,906	7.1	62,880	33	8,496	4.5
8125	69	F	3	53.9	153	2,672	18.53	132,265	49.5	62,633	23.5

cNF, cutaneous neurofibromas; F, female; M, male.

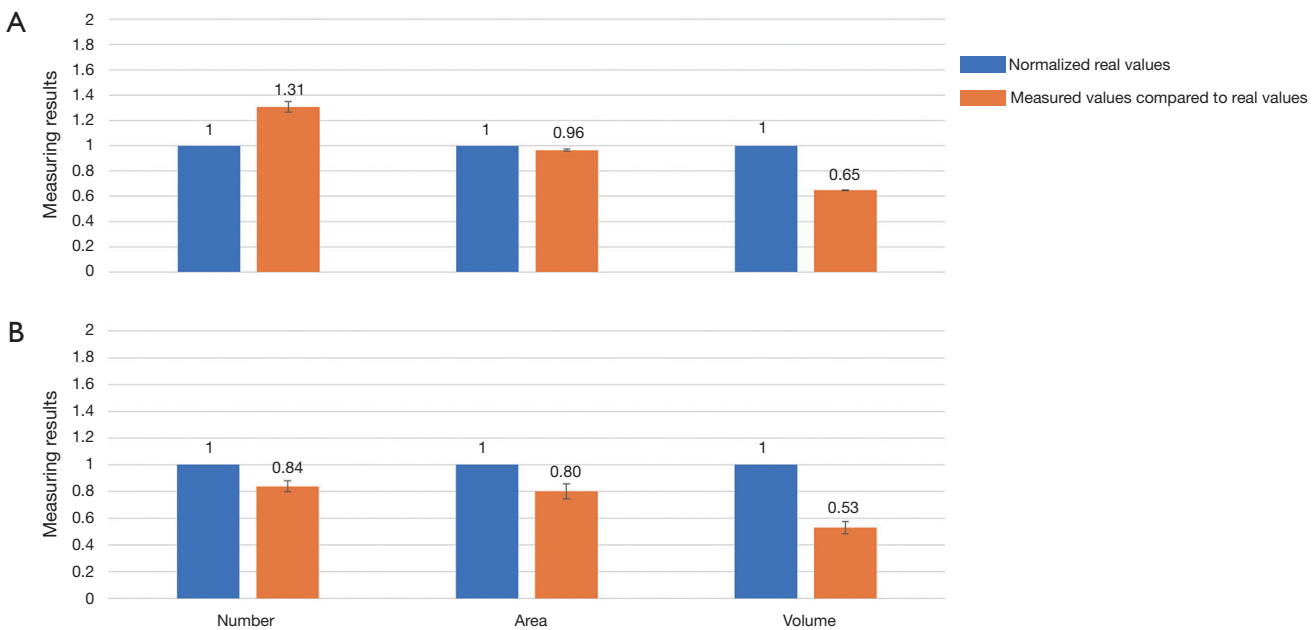

Figure 2 Measuring results on spheres. Number, total area, and total volume of the hemispheres were normalized to the real ones, respectively. (A) Evenly distributed; (B) clustered.

Table 2 Comparison of measured and reference values for area and volume of model neurofibromas (scenario 1), including the variation coefficient and standard deviation

Indices	Number	Area	Volume
Number of measurements	5	5	5
Average	130.6	22,918.2 mm^2	39,087.6 mm^3
Standard deviation	4.72	200.29 mm^2	178.73 mm^3
Reference	100	23,752.97 mm^2	60,409.08 mm^3
Variation coefficient	3.62%	0.87%	0.46%

Table 3 Comparison of measured and reference values for area and volume of model neurofibromas (scenario 2), including the variation coefficient and standard deviation

Indices	Number	Area	Volume
Number of measurements	5	5	5
Average	83.8	19,001.61 mm^2	31,965.84 mm^3
Standard deviation	4.55	1,479.42 mm^2	3,056.53 mm^3
Reference	100	23,752.97 mm^2	60,409.08 mm^3
Variation coefficient	5.43%	7.78%	9.56%

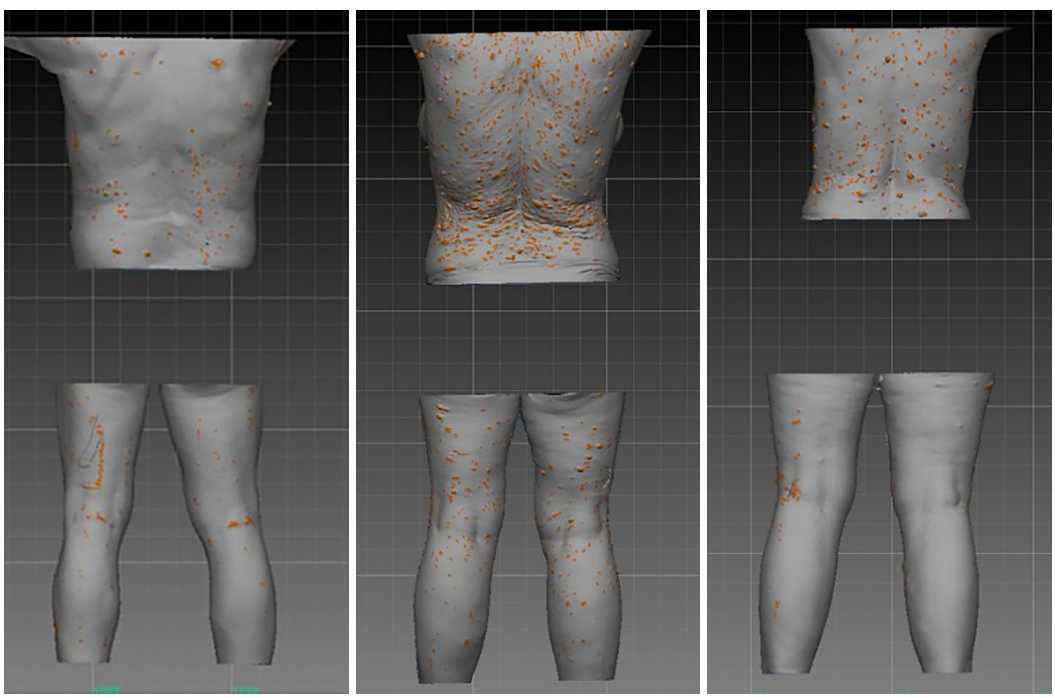

Figure 3 Three examples of the scanner detecting cNF on backs and legs of patients. This image is published with the participants' consent. cNF, cutaneous neurofibromas.

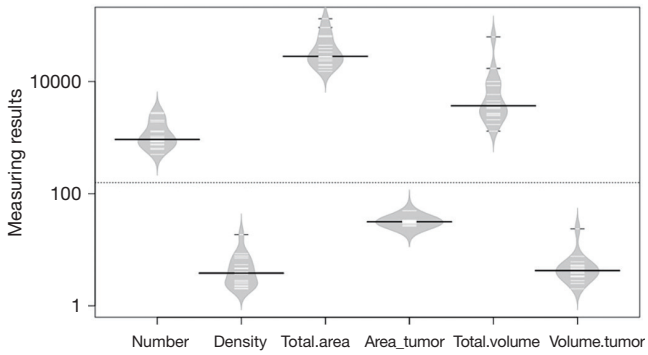

Figure 4 Measuring results from the 16 patients. Density is the ratio of fibroma area/total area. Areas are in mm^2. Volumes are in mm^3.

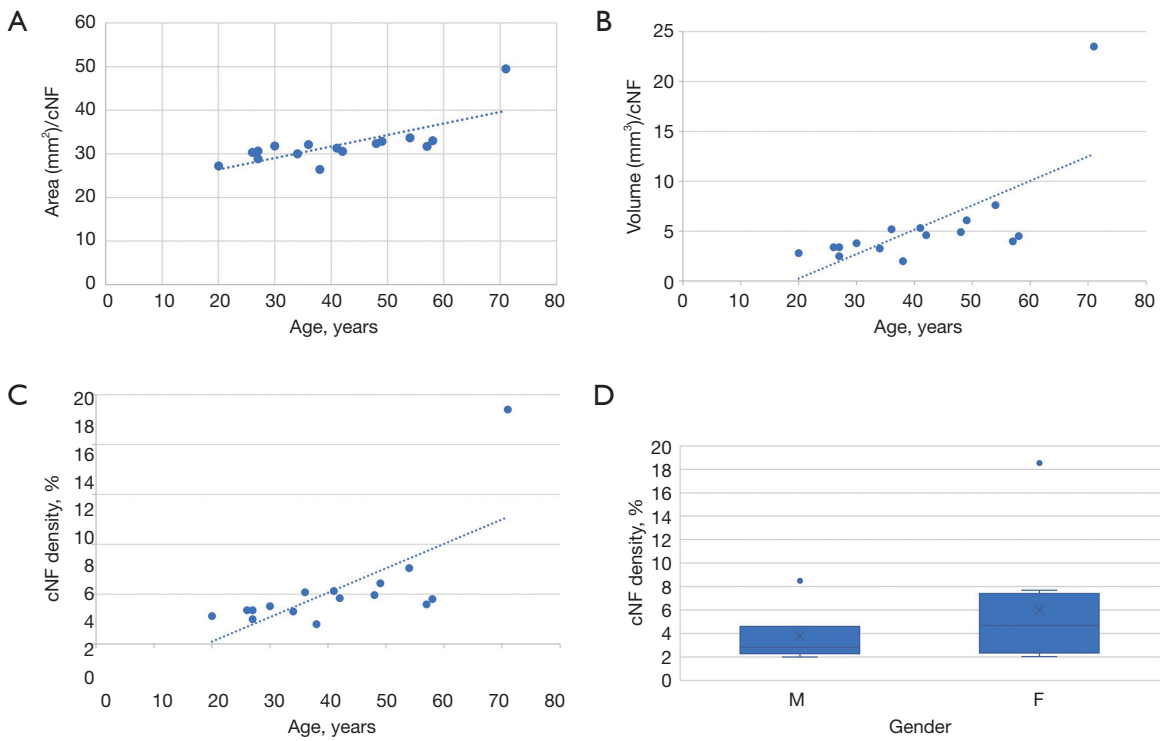

Figure 5 Measured parameters in correlation with age (A-C) and gender (D) of the patients. cNF, cutaneous neurofibromas; F, female; M, male.

(*Figure 7D*), which leads to an underestimation of all three parameters: number, area, and volume. However, these weaknesses can be overcome with improvements in the analysis software. For example, adding a water-washing function to separate clustered tumors.

Several studies have highlighted the importance of sensitive and reproducible methods for quantifying cNF. Traditional approaches, such as manual counting or caliper measurements, show considerable inter- and intrarater variability and are therefore limited in their ability to detect subtle changes over time (16,17). Imaging-based techniques, including ultrasound and 3D imaging, have been shown to provide improved reliability and sensitivity for documenting cNF burden in clinical studies (16,17). In particular, comparative analyses of 3D imaging systems demonstrate high reliability for surface-based parameters such as lesion area, whereas volumetric measurements tend to show greater variability between devices (18), which is consistent

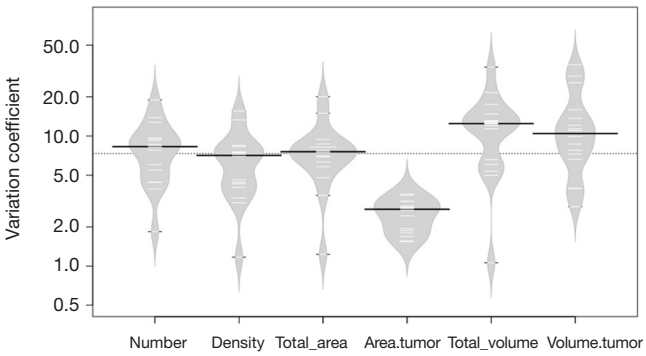

Figure 6 Variation coefficients for the parameters measured in 15 or 30 scans.

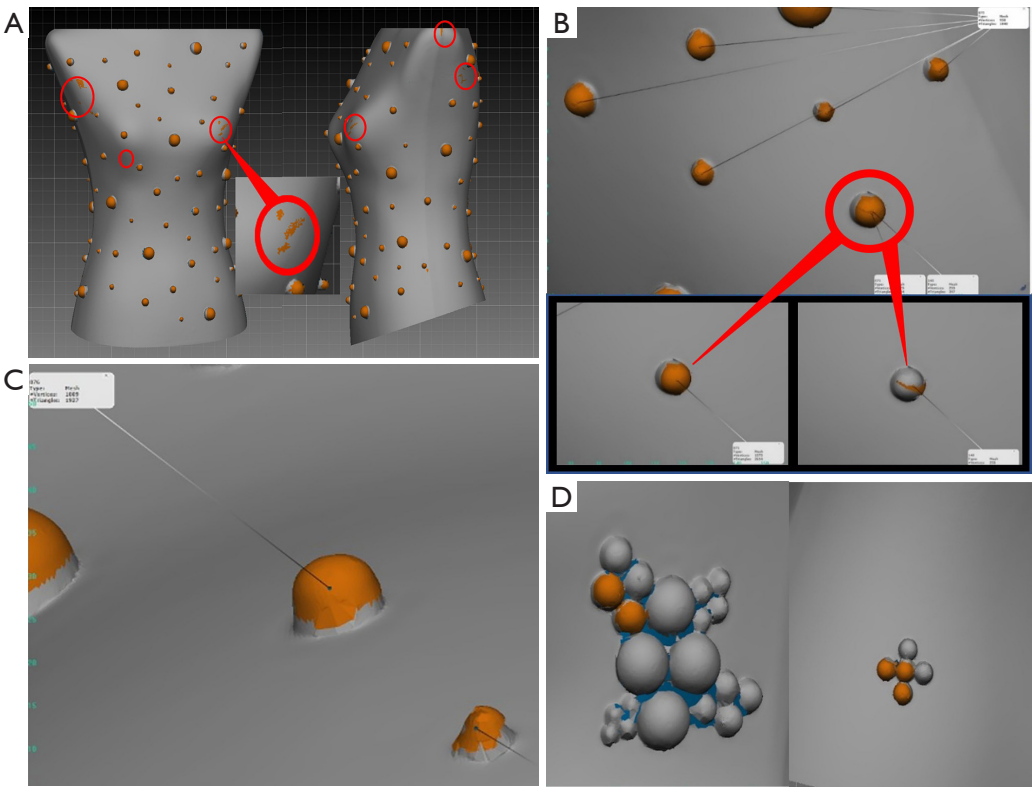

Figure 7 Over- and underestimation in the measurement of the hemisphere model. (A) Artefactual areas captured as hemispheres (circles) leading to overestimation of the total number; (B) a hemisphere captured twice as a whole and as fragment (circle), leading to overestimation of the total number; (C) incomplete capture of hemisphere near the border leading to underestimation of area and volume; (D) hemispheres with contact to each other captured as a single one, leading to underestimation of total number.

with the variability observed in our measurements.

The major advantages of SL 3D scanners are the fast capturing over the entire body surface and the low cost (27). For comparison, whole-body MRI is far more expensive and cannot be used for routine documentation. In addition, whole-body MRI does not have the sensitivity for small and superficial tumors. Another comparison is with laser-based point-by-point scanning, which is accurate but expensive and time-consuming (24,28). Additionally, laser scanners use high-powered lasers, which is potentially hazardous and

therefore not suitable for application on the human body.

Another advantage of the scanner is that the scanning process does not involve physical contact, which is more comfortable for the patients. Upon further development, we hope that the operation of the scanner to be constructed in such a simple way that a patient can start the measurement by himself, leading to more protected privacy and also time savings for the medical professional. The described measurement method demonstrates high reliability, as evidenced by the consistency of results and a relatively low standard deviation. While the measurements deviate from the true value, the underlying error causing this deviation is consistently reproduced across measurements, indicating systematic bias. Despite this limitation, the method provides reproducible results, making it particularly well-suited for comparisons or relative measurements where consistency holds greater importance than absolute accuracy.

Using this scanner, we have obtained real results from 16 patients, which are in concordance with our expectations and with the reported observation: density, total area, and total volume of the neurofibromas increase with age (8,9,13). In addition, we found that the average area per tumor also increases with age, suggesting that neurofibromas not only increase in number but also grow in size.

Conclusions

Our NF-scanner offers a method for quantifying a large number of cNF with several advantages over conventional imaging techniques like MRI or manually counting. With further optimization, especially in the analysis software, the scanner is expected to find its value for clinical documentation and studies.

Acknowledgments

We would like to thank our patients for their valuable cooperation in this study. Parts of this article were presented and published in the form of a poster presentation at the 98th Congress of the German Society of Neurology.

Footnote

Reporting Checklist: The authors have completed the STARD reporting checklist. Available at https://qims.amegroups.com/article/view/10.21037/qims-2026-1-0053/rc

Data Sharing Statement: Available at https://qims.amegroups.com/article/view/10.21037/qims-2026-1-0053/dss

Funding: This work was supported by the Bundesverband Neurofibromatose.

Conflicts of Interest: All authors have completed the ICMJE uniform disclosure form (available at https://qims.amegroups.com/article/view/10.21037/qims-2026-1-0053/coif). T.I.H. received speaker honoraria and compensation for advice or lecturing from Alexion, not related to this study. S.C.F. received speaker honoraria from AstraZeneca and Alexion, and compensation for advice or lecturing from Alexion, not related to this study. The other authors have no conflicts of interest to declare.

Ethical Statement: The authors are accountable for all aspects of the work in ensuring that questions related to the accuracy or integrity of any part of the work are appropriately investigated and resolved. The study was conducted in accordance with the Declaration of Helsinki and its subsequent amendments. The study was approved by the ethics committee of Ärztekammer Hamburg, Germany (Nos. 2022-300264-WF and 2022-100983-BO-ff), and informed consent was taken from all individual participants.

References

1. Uusitalo E, Leppävirta J, Koffert A, Suominen S, Vahtera J, Vahlberg T, Pöyhönen M, Peltonen J, Peltonen S. Incidence and mortality of neurofibromatosis: a total population study in Finland. J Invest Dermatol 2015;135:904-6.
2. Legius E, Messiaen L, Wolkenstein P, Pancza P, Avery RA, Berman Y, et al. Revised diagnostic criteria for neurofibromatosis type 1 and Legius syndrome: an international consensus recommendation. Genet Med 2021;23:1506-13.
3. Gutmann DH, Ferner RE, Listernick RH, Korf BR,

Wolters PL, Johnson KJ. Neurofibromatosis type 1. Nat Rev Dis Primers 2017;3:17004.
4. Hofmann S, Winkler S, Baumann M, Zellner H. Quality of Life in Children and Adolescents with Neurofibromatosis Type 1: A Single-Center Observational Study. Neuropediatrics 2023;54:430-2.
5. Yoo HK, Porteous A, Ng A, Haria K, Griffiths A, Lloyd A, Yang X, Kazeem G, Barut V. Impact of neurofibromatosis type 1 with plexiform neurofibromas on the health-related quality of life and work productivity of adult patients and caregivers in the UK: a cross-sectional survey. BMC Neurol 2023;23:419.
6. Wolkenstein P, Zeller J, Revuz J, Ecosse E, Leplège A. Quality-of-life impairment in neurofibromatosis type 1: a cross-sectional study of 128 cases. Arch Dermatol 2001;137:1421-5.
7. Huson SM, Harper PS, Compston DA. Von Recklinghausen neurofibromatosis. A clinical and population study in south-east Wales. Brain 1988;111:1355-81.
8. Dugoff L, Sujansky E. Neurofibromatosis type 1 and pregnancy. Am J Med Genet 1996;66:7-10.
9. Duong TA, Bastuji-Garin S, Valeyrie-Allanore L, Sbidian E, Ferkal S, Wolkenstein P. Evolving pattern with age of cutaneous signs in neurofibromatosis type 1: a cross-sectional study of 728 patients. Dermatology 2011;222:269-73.
10. Plotkin SR, Bredella MA, Cai W, Kassarjian A, Harris GJ, Esparza S, Merker VL, Munn LL, Muzikansky A, Askenazi M, Nguyen R, Wenzel R, Mautner VF. Quantitative assessment of whole-body tumor burden in adult patients with neurofibromatosis. PLoS One 2012;7:e35711.
11. Well L, Careddu A, Stark M, Farschtschi S, Bannas P, Adam G, Mautner VF, Salamon J. Phenotyping spinal abnormalities in patients with Neurofibromatosis type 1 using whole-body MRI. Sci Rep 2021;11:16889.
12. Ristow I, Kaul MG, Stark M, Zapf A, Riedel C, Lenz A, Mautner VF, Farschtschi S, Apostolova I, Adam G, Bannas P, Salamon J, Well L. Discrimination of benign, atypical, and malignant peripheral nerve sheath tumors in neurofibromatosis type 1 using diffusion-weighted MRI. Neurooncol Adv 2024;6:vdae021.
13. Cannon A, Chen MJ, Li P, Boyd KP, Theos A, Redden DT, Korf B. Cutaneous neurofibromas in Neurofibromatosis type I: a quantitative natural history study. Orphanet J Rare Dis 2018;13:31.
14. Cunha KS, Rozza-de-Menezes RE, Andrade RM, Theos A, Luiz RR, Korf B, Geller M. Validity and interexaminer reliability of a new method to quantify skin neurofibromas of neurofibromatosis 1 using paper frames. Orphanet J Rare Dis 2014;9:202.
15. Lin MJ, Yao H, Vera K, Patel E, Johnson M, Caroline P, Ramos J, Mehta J, Hu X, Blakeley JO, Romo CG, Sarin KY. Cutaneous Neurofibromas and Quality of Life in Adults With Neurofibromatosis Type 1. JAMA Dermatol 2024;160:1091-8.
16. Thalheimer RD, Merker VL, Ly KI, Champlain A, Sawaya J, Askenazi NL, Herr HP, Da JLW, Jordan JT, Muzikansky A, Pearce EM, Sakamoto FH, Blakeley JO, Anderson RR, Plotkin SR; REiNS International Collaboration. Validating Techniques for Measurement of Cutaneous Neurofibromas: Recommendations for Clinical Trials. Neurology 2021;97:S32-41.
17. Li Y, Blakeley JO, Ly I, Berman Y, Lau J, Wolkenstein P, Bergqvist C, Jia W, Milner TE, Katta N, Durkin AJ, Kennedy GT, Rowland R, Romo CG, Fleming J, Kelly KM. Current and Emerging Imaging Techniques for Neurofibromatosis Type 1-Associated Cutaneous Neurofibromas. J Invest Dermatol 2023;143:1397-405.
18. Lau JCL, Fleming J, Good M, Lim A, Saunderson RB, Phan TA, Schlub T, Siow SF, Lacson N, Romo C, Blakely J, Bergqvist C, Berman YD. Comparing 3D imaging devices for the measurement of cutaneous neurofibromas in patients with Neurofibromatosis Type 1. Skin Res Technol 2024;30:e70020.
19. Cannon A, Pichard DC, Wolters PL, Adsit S, Erickson G, Lessing AJ, Li P, Narmore W, Röhl C, Rosser T, Widemann BC, Blakeley JO, Plotkin SR; REiNS International Collaboration. Perspective of Adults With Neurofibromatosis 1 and Cutaneous Neurofibromas: Implications for Clinical Trials. Neurology 2021;97:S15-24.
20. Geng J. Structured-light 3D surface imaging: a tutorial. Adv Opt Photonics 2011;3:128-60.
21. Rieke-Zapp D, Royo S. Structured light 3D scanning. In: Bentkowska-Kafel A, MacDonald L, editors. Digital techniques for documenting and preserving cultural heritage. 1st ed. Leeds: Arc Humanities Press; 2017:247-51.
22. McPherron SP, Gernat T, Hublin JJ. Structured light scanning for high-resolution documentation of in situ archaeological finds. Journal of Archaeological Science 2009;36:19-24.
23. Grazioso S, Selvaggio M, Di Gironimo G. Design and development of a novel body scanning system for healthcare applications. Int J Interact Des Manuf

2018;12:611-20.
24. Bartol K, Bojanić D, Petković T, Pribanić T. A review of body measurement using 3D scanning. IEEE Access 2021;9:67281-301.
25. Cutti AG, Santi MG, Hansen AH, Fatone S; Residual Limb Shape Capture Group. Accuracy, Repeatability, and Reproducibility of a Hand-Held Structured-Light 3D Scanner across Multi-Site Settings in Lower Limb Prosthetics. Sensors (Basel) 2024;24:2350.
26. Ahlawat S, Blakeley JO, Langmead S, Belzberg AJ, Fayad LM. Current status and recommendations for imaging in neurofibromatosis type 1, neurofibromatosis type 2, and schwannomatosis. Skeletal Radiol 2020;49:199-219.
27. Haleem A, Javaid M. 3D scanning applications in medical field: a literature-based review. Clinical Epidemiology and Global Health 2019;7:199-210.
28. Frisky AZK, Fajri A, Brenner S, Sablatnig R. Acquisition Evaluation on Outdoor Scanning for Archaeological Artifact Digitalization. In: Proceedings of the 15th International Joint Conference on Computer Vision, Imaging and Computer Graphics Theory and Applications (VISIGRAPP 2020). 2020:792-9.

Cite this article as: Hartung TI, Dinga GT, Butschan J, Kluwe L, Farschtschi SC. Quantitative measurement of cutaneous neurofibromas in neurofibromatosis type 1 using a structured-light scanner. Quant Imaging Med Surg 2026;16(6):478. doi: 10.21037/qims-2026-1-0053